


## Facile synthesis and catalytic evaluation of iron-doped zinc oxide nanocatalysts for biodiesel production

Jaffar Hussain<sup>1\*</sup>, Zeenat Muhammad Ali<sup>1</sup>, Farman Ali Shah<sup>1</sup>,  
Abdul Qadeer<sup>1</sup> , Abdul Nasir Laghari<sup>2</sup>, Munazza Sohail<sup>3</sup>

<sup>1</sup> Department of Chemical Engineering Mehran University of Engineering and Technology, Jamshoro, 76062, Pakistan

<sup>2</sup> Department of Chemical Engineering Quaid-e-Awam University of Engineering Science and Technology Nawabshah, Pakistan

<sup>3</sup> Pakistan Council of Scientific and Industrial Research (PCSIR) Karachi, Pakistan

\* Corresponding author's e-mail: jafarkhosa72@yahoo.com

### ABSTRACT

The global transition in energy consumption patterns driven by the depletion of fossil fuel reserves, rapid population growth, and increasing environmental pollution has faster the exploration for renewable and ecological energy substitutes. Among these, biodiesel has materialized as a capable candidate due to its carbon-neutral profile, environmental compatibility, and potential as a cleaner alternate for conventional petroleum-based diesel. In this study, the performance of iron(II)-doped zinc oxide (Fe(II)-ZnO) nanocatalyst was investigated for biodiesel production from *Jatropha curcas* oil. The nanocatalyst was synthesized and characterized using atomic force microscopy (AFM), fourier transform infrared spectroscopy (FTIR), x-ray diffraction (XRD), and zeta potential analysis. AFM analysis revealed pronounced surface topography with elevated features reaching up to 50 nm in height. The formation of Zn–O and Fe–O bonding was affirmed through FTIR spectra, while XRD analysis demonstrated the presence of crystalline phases corresponding to Fe<sub>2</sub>O<sub>3</sub> and ZnO, with the most intense diffraction peak observed at  $2\theta = 35.8777^\circ$ . Zeta potential measurements indicated moderate colloidal stability with a measured value of  $-4.01$  mV. The *Jatropha curcas* oil used in the transesterification process possessed a density of 909 kg/m<sup>3</sup> at 25 °C, an acid value of 1.20 mg KOH/g, and a viscosity of 25.63 mm<sup>2</sup>/s.. Transesterification was carried out under optimized reaction conditions, comprising a methanol-to-oil molar ratio of 12:1, reaction temperature of 50 °C, catalyst loading of 2% Fe(II)-ZnO, and a reaction time ranging from 10 to 180 minutes. The produced biodiesel exhibited a density within the ASTM D6751 standard specifications. While the flash point was slightly elevated making it suitable for blending with petro-diesel the viscosity remained marginally higher than standard diesel fuel.

**Keywords:** nanoparticle, renewable energy, iron oxide, nanocatalyst, biodiesel.

### INTRODUCTION

Biodiesel is a renewable fuel which contain mono-alkyl esters resulting from long-chain fatty acids, typically sourced from vegetable oils or animal fats. Its sustainable nature and lower emissions of greenhouse gases and particulate matter make it a strong alternative to conventional diesel. Additional benefits include excellent lubricating properties, a high cetane number, elevated flash point, and significant biodegradability. While edible oils have been examined for biodiesel

production, their cost-intensive feature presents a substantial barrier. Therefore, researchers have started diverting their attention to more affordable alternatives, like non-edible oils *Jatropha curcas* and waste cooking oils. Oil yield is one of key factors considered in choosing an appropriate biodiesel feedstock. It is believed that the crops producing higher quantity of oil are preferred due to lower production costs [Baskar and Soumiya, 2016]. Biodiesel is produced *via* transesterification, which involves triglycerides and alcohol reacted in the presence of a nanocatalyst. During

this reaction, fatty acid and methyl esters (FAME) are generated while the glycerol results as a by-product. Common alcohols used in this reaction are methanol and ethanol, Brayko et al. [2018]. *Jatropha* oil, can be considered one of the most promising sources. Its high ricinoleic acid content characterized by the presence of a hydroxyl group contributes to its naturally high density and viscosity. These properties, together with its solubility in alcohol, have significant effect on the efficiency of transesterification process, Hara et al. [2009]. Homogeneous and heterogeneous catalysts are used for the production of bioethanol. Heterogeneous ones are more efficient because of due to their reusability and ease of separable, making them proper for both batch and continuous operations. Nowadays, nanocatalysts have attracted considerable interest, owing to their high surface area and catalytic efficiency. Their easy separation from reaction products further enhances their industrial appeal, according to Kirubakaran et al. [2018]. In industrial applications, heterogeneous catalysts are especially valued for their selectivity and simple post-reaction separation. Nanomaterials, known for their tunable and unique surface properties, have gained significant attention across a wide range of applications [Damian et al., 2025; Das, 2025; Krawczyk et al., 1996; Rajagopal, 2007; Sathish and Viswanath et al., 2007; Sharma, et al 2018; Sharma, et al., 2018; Sudhagar et al., 2008], making them highly suitable for catalyzing biodiesel production. In recent years, several nano-sized heterogeneous catalysts have been investigated for use in the transesterification process [Yuan et al., 2014; Teo et al., 2018; Yousefi et al., 2018; Gardy et al., 2018; Yuan et al., 2014; Hussain, 2022; Hussain, 2023]. However, many of these processes still require extended reaction times (3–9 hours) and elevated temperatures (65–120 °C), which can hinder efficiency.

To overcome these limitations, in the current research Fe(II) doped ZnO and its composites were developed, which are capable of accelerating the transesterification reaction at lower temperatures, while also offering easy separation after the reaction. Fe(II) doped ZnO and its composites have shown promise in this regard, due to their ability to retain essential properties even after repeated catalytic cycles. Fe(II) doped ZnO achieving cost-effective catalyst recovery and reuse without compromising the integrity or activity of the active sites of the catalyst. The significant

contribution of this work emerges from use of locally grown *Jatropha curcas* extracted oil as a renewable, low-cost, and abundant resource. Moreover, Fe(II) doped ZnO shows multifunctionality combining fast catalytic activity, cost-effective, catalyst recovery and reuse without compromising the integrity, making it an ecological, cost-effective, and easily retrievable catalyst for the bioethanol production.

## MATERIALS AND METHODS

### Materials and reagents

All chemicals, such as ZnO and Fe sulfates, NaOH, and methanol for the transesterification reaction were bought from local market of Hyderabad Al-Beruni scientific store of sigma Erich chemicals supplier company.

### Fabrication of iron (II)-ZnO nanocatalyst

Fe(II) doped ZnO nanocatalyst was fabricated using the co-precipitation method described by Sampa et al. [2015]. Initially, appropriate quantities of zinc and ferrous sulfate were disbanded in double distilled water (DDW) to form sol-A, subjected to ultrasonic treatment at a frequency of 57 kHz for two hours, followed by continuous stirring at room temperature using a magnetic stirrer. In parallel, a 0.5 M sodium hydroxide (NaOH) solution (Sol-B) was set using DDW. Sol-B was slowly added to Sol-A till the pH of the mixture reached 12. The resulting mixture was then stirred continuously for an additional 30 minutes. The solution was left to age at room temperature for 18 hours. After aging, the precipitate was separated by centrifugation and washed repeatedly with ethanol and DDW to eliminate any remaining contaminations. The obtained solid was dried in an oven at 200 °C for one hour, resulting in a brown-colored powder of Fe(II) doped ZnO nanocomposite. Finally, the dried product was calcinated at 700 °C to enhance crystallinity.

### Fe (II)-ZnO nanocatalyst characterization

Morphological features of synthesized Fe (II) doped ZnO nanocatalyst was characterized by scanning electron microscopy (SEM), x-ray diffraction (XRD) were employed evaluate the crystalline size and phase composition. Functional

groups and species adsorbed on the catalyst surface were investigated through fourier transform infrared spectroscopy (FTIR) while the atomic force microscopy (AFM) technique was applied to assess the average grain size and surface roughness of catalyst. Moreover, Gas chromatography-mass spectrometry (GC–MS) investigation was implemented to estimate the finally produced biodiesel and fatty acid profile.

### Transesterification of *Jatropha curcas* oil

The transesterification of *Jatropha curcas* oil was conducted in a batch process using a 500 mL beaker equipped with a magnetic stirrer and a heating plate. To begin, the required amount of catalyst was thoroughly mixed with methanol in the beaker. Subsequently, a pre-measured quantity of *Jatropha* oil was added to the methanol–catalyst mixture. The amount of catalyst used was determined based on its weight ratio relative to the oil (g catalyst/g oil). The reaction mixture was heated to the desired temperature and maintained under continuous stirring or left undisturbed depending on the experimental conditions and the reaction time. After the specified reaction period, the resulting solution was shifted for extraction in separating funnel and allowed to settle for approximately 2 hours to facilitate the separation of the product layers. The denser glycerol phase settled at the bottom and was carefully removed, while the upper biodiesel phase was collected, washed with warm distilled water to remove impurities, and then dried and measured for yield. The residual catalyst at the bottom of the reaction vessel was carefully collected, regenerated, and

reused in subsequent cycles to evaluate its reusability. Transesterification reactions were carried out by varying key process variables such as concentration of catalyst (2–18%), methanol to oil molar ratio (5:1 to 14:1), reaction time (10–180 minutes), and temperature (40–60 °C).

The final biodiesel product consisted primarily of fatty acid methyl esters, along with minor components such as monoglycerides, diglycerides, and unreacted triglycerides. These components were identified and computed using gas chromatography coupled with mass spectrometry (GC–MS), and the biodiesel yield or conversion efficiency was subsequently calculated.

$$\text{Biodiesel conversion (\%)} = \frac{\text{Total amount of biodiesel obtained}}{\text{Total amount of Jatropha Oil used}} \times 100 \quad (1)$$

### Properties of *Jatropha carcus* oil

Before transesterification the properties of *Jatropha curcas* oil was determined through gas chromatograph analyses shown in Table 1, 2 and Figure 1. The reaction parameters were optimized by varying experimental conditions. Table 3 demonstrated the optimized parameters.

## RESULTS AND DISCUSSION

### Characterization

#### Atomic force microscopy (AFM)

The synthesized Fe(II)-ZnO characterized by AFM at HEJ Research Institute of Chemistry, Karachi. AFM is a versatile imaging technique

**Table 1.** Physical properties of *Jatropha carcus* oil

Acid value (mg KOH/gm)	Density (kg/m <sup>3</sup> )	Viscosity (Cst)	Flash point (°C)
1.20	909 at 25°C	25.63	250

**Table 2.** The gas chromatographic analysis of *Jatropha carcus* oil

Fatty acid (weight %)				
Olic acid	Palmitic acid	Linoleic acid	Stearic acid	Linolenic acid
70.6	15	7.9	1.8	0.6

**Table 3.** Optimized experimental condition for biodiesel production with Fe(II) doped ZnO

<i>Jatropha curcas</i> oil to methanol (molar ratio)	Temperature (°C)	Reaction time (min)	Catalyst to <i>Jatropha curcas</i> oil (g)
1:12	50	150	2

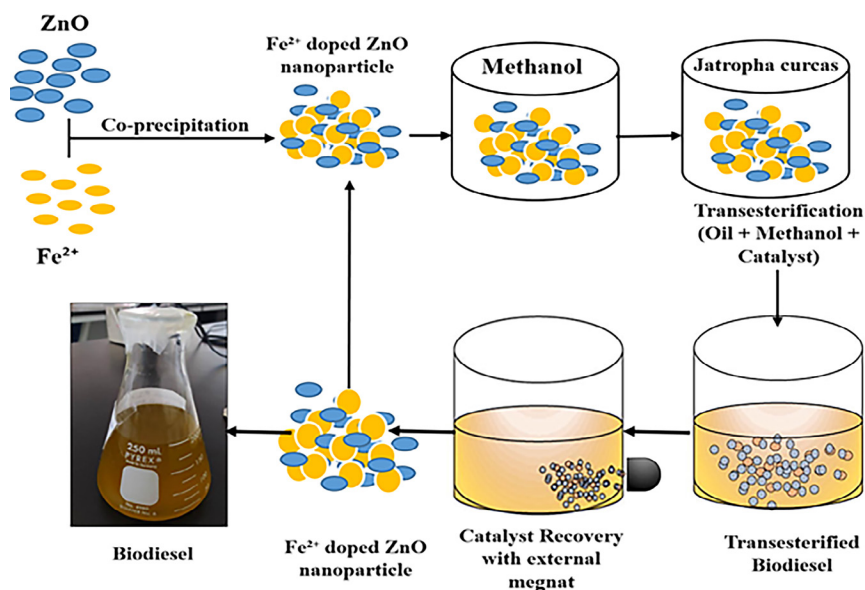


**Figure 1.** Schematic diagram of production of biodiesel from *Jatropha curcas* oil Fe(II) doped ZnO

that provides 3D topographical information and insights into the mechanical properties of surfaces at the nanoscale. In this study, a Veeco AFM (model Nano Scope IIIa) equipped with a liquid cell and integrated with an automated syringe pump was used. AFM captured 2D and 3D images of the nanocatalyst, revealing distinct elevated features and elevated smooth surface structures resembling bumps. (Figure 2). The image space was 25  $\mu\text{m}$ , 251  $\mu\text{m}$ , 52.4  $\mu\text{m}$  on x, y, and z axis, respectively, reveal elevated and distinct features, with heights varying up to about 50 nm.

### Fourier transform infrared spectroscopy FTIR

FTIR allows for the identification of specific functional groups within the sample, proving particularly valuable for identifying acidic sites in Fe(II)-ZnO. FTIR spectra exhibited stretching vibrations between 500–800  $\text{cm}^{-1}$  characteristic of Fe-O or Zn-O bonds. The peaks in the 1000–1500  $\text{cm}^{-1}$  region are attributed to metal-oxygen bonds or O-H groups. A strong band at 1650  $\text{cm}^{-1}$  indicated the presence of adsorbed water molecules (Figure 3).

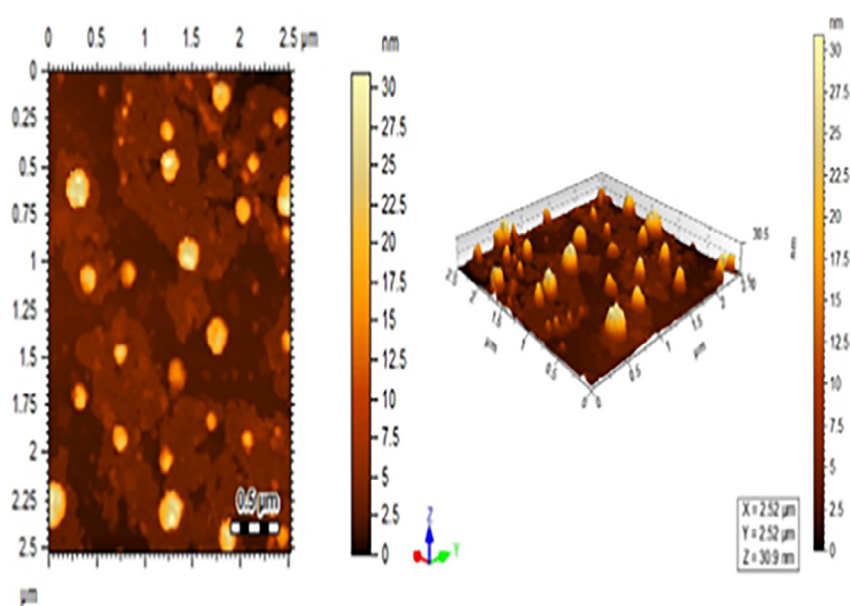


**Figure 2.** Atomic force microscopy of Fe(II) doped ZnO

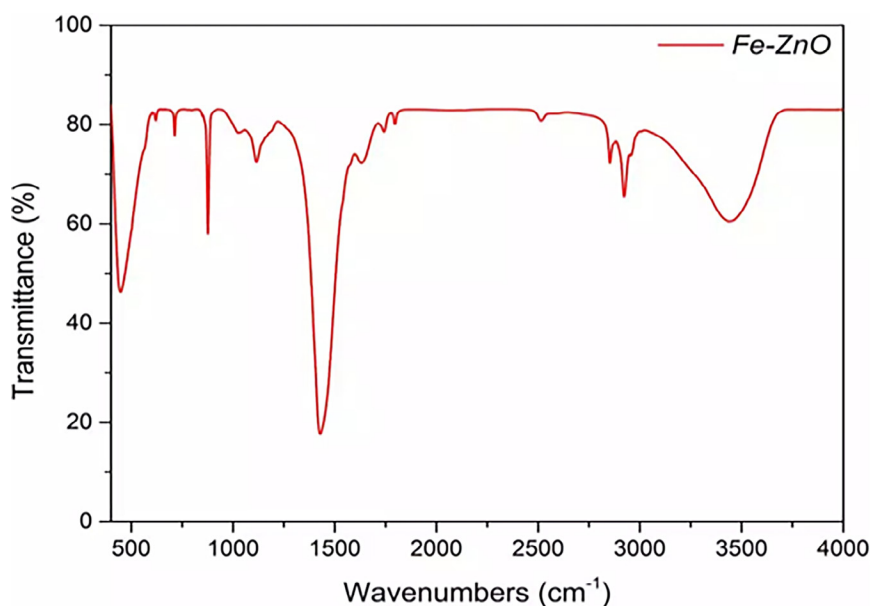


Figure 3. Fourier transform infrared spectroscopy of Fe(II) doped ZnO

### Zeta potential

Zeta potential is used to assess the stability of colloidal suspensions. A high zeta potential signifies strong interparticle repulsion and a stable suspension, while a low zeta potential indicates instability. Factors like ionic strength and pH influence zeta potential. This technique is essential for determining surface charge and stability, as illustrated by zeta potential measurements same. Zeta potential is negative 4.01 mv, zeta deviation is 3.93 and caducity 0.0251 (Figure 4).

### X-ray diffraction (XRD)

X-ray diffraction (XRD) analysis, a non-destructive technique for characterizing crystalline materials, was performed using Bruker Germany equipment (Figure 5). The analysis

revealed distinct peaks corresponding to ZnO and  $\text{Fe}_2\text{O}_3$  phases. The peak with the highest intensity (141.4926) at  $35.8777^\circ$  had a d-spacing of 2.503 Å and a relative intensity of 100%. This indicates the presence of highly crystalline hydrotalcite.

The biodiesel produced undergoes analysis in PCSIR lab Complex and Wuhan golden wing industry (Table 4).

Biodiesel exhibits a slightly elevated acid value above the recommended 0.5 mg KOH/g, posing a risk of engine corrosion, deposits, and potential catalyst deactivation. While its density falls within the ASTM recommended range (870–900 kg/m<sup>3</sup> at 15 °C), suggesting good engine compatibility in blends, its higher viscosity (typically 2.5–5 cSt is permissible limit) affects fuel flow and injection system efficiency. Although acceptable, the borderline acid value needs attention, as it can also impact fuel stability, promoting gum

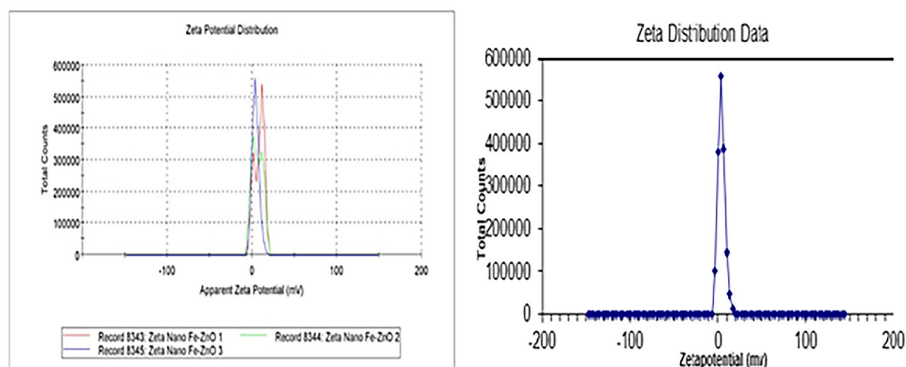


Figure 4. Zeta potential of Fe(II) doped ZnO

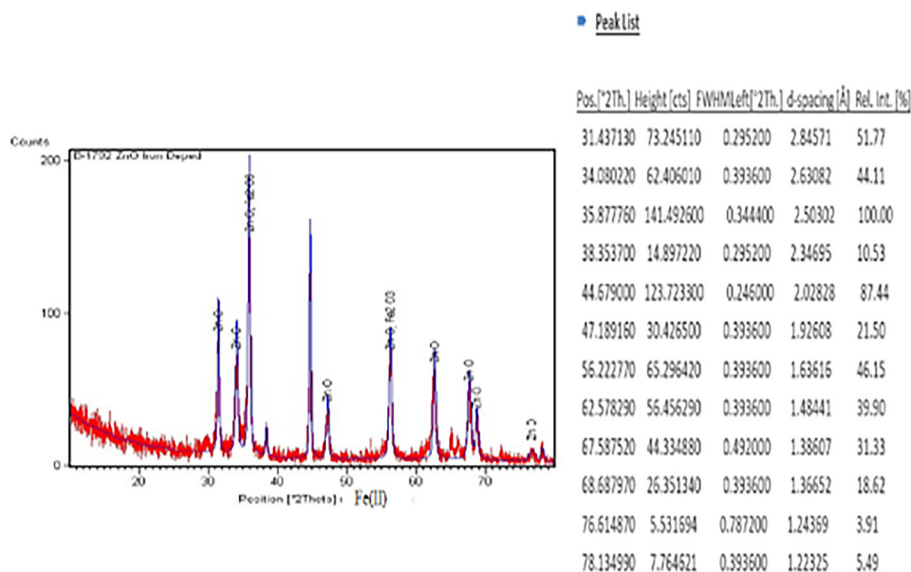


Figure 5. X-ray diffraction of Fe(II) doped ZnO

Table 4. Testing of produced biodiesel with Fe(II) doped ZnO

Test	Equipment name	Equipment model	Testing method	Limit	Synthesized biodiesel	Parameter
Density at 40 °C (kg/m <sup>3</sup> )	Weight (Rd bottle/ balance)	Av-65	ASTM D4052	860–900	884	PCSIR laboratory
Viscosity at 40 °C (Cst)	Viscometer	Kv.6 Viscometer UK	ASTM D	0.5–5.0	13.09	
Acid value (mg KOH/g )	Titration method	–	ASTM D664	0.8	0.5207	
Flash point (°C)	Close up flash point tester	FP Tester13661.4	ASTMD93	130	148	
Oil composition	Gas chromatograph	Gc: 7890B	Mass spectra	–	–	Wuhan golden wing industry

formation and sedimentation. The flash point, crucial for safe handling and storage, was also assessed. The quantity analysis reveals that biodiesel recovery was 98.5%.

### Comparison of present study with available researchers

To evaluate the catalytic efficiency of the synthesized Fe(II)-doped ZnO, its performance was compared with various reported metal oxides

and doped metal oxide catalysts utilized in biodiesel production, as summarized in Table 5. The Fe(II)-doped ZnO catalyst demonstrated superior activity, achieving a high conversion efficiency of 98.5% within a reduced reaction time and very catalyst dose, thereby outperforming several reported counterparts. Safaripour et al. [2023]. reported a LaNiO<sub>3</sub>-based perovskite catalyst which exhibited a conversion efficiency of 95.14% over a reaction time of 180 minutes. Kumar et al. [2020] employed a Li-CaO solid base catalyst derived

Table 5. Comparison of current study with available literature

Catalyst	Time (min)	Temperature (°C)	Methanol/oil molar ratio	Catalyst amount (%)	Conversion (%)	Reference
Fe <sup>2+</sup> ZnO	150	50	1:12	2	98.5	This work
ZnO	180	65	30	6	96.5	Darvishvand et al (2024)
Sm-LaNiO <sub>3</sub>	180	80.07	9.07	3.08	95.14	Safaripour et al., (2023)
Li-CaO	150	65	15	4	97.8	Kumar and Gupta (2020)
Na-CaO	210	60	6	3	83.57	Kurniawan et al., (2020)

from *Musa balbisiana* root oil, which achieved a biodiesel yield of 97.8% in 150 minutes. Additionally, Kurniawan et al. [2020] synthesized a Na-doped CaO catalyst, resulting in a conversion of 83.57% after 210 minutes of reaction time. In contrast, the Fe(II)-doped ZnO catalyst developed in the present study not only facilitated a higher conversion rate, but also significantly reduced the required reaction time, highlighting its enhanced catalytic performance and potential as an efficient heterogeneous catalyst for biodiesel production via transesterification.

## CONCLUSIONS

Scaling up biodiesel production requires catalysts that are energy-efficient to synthesize, promote fast transesterification, and offer easy reusability. In this study, Fe(II) doped ZnO composites were successfully synthesized and characterized using multiple analytical techniques. The transesterification process was completed within 150 minutes hours, 50 °C and 2% catalyst dose, yielding biodiesel rich in C18 methyl esters. Notably, the Fe(II) doped ZnO nanoparticles exhibited soft ferromagnetic properties, with high magnetization and low coactivity, allowing for rapid and effortless magnetic separation using a low magnetic field. These nanoparticles demonstrated a recovery efficiency of approximately  $90 \pm 2\%$  and maintained high catalytic activity upon reuse. Given these promising features, Fe(II) doped ZnO nanocomposite present a strong potential as a reusable catalyst for biodiesel production. However, further optimization of reaction parameters, dopant levels, and feedstock types is necessary for effective large-scale application.

## Acknowledgements

Authors highly acknowledge the facilities provided the department of geology university of Sindh and chemical engineering for the characterization of samples.

## REFERENCES

1. Baskar, G., Soumiya, S. (2016). Production of biodiesel from castor oil using iron (II) doped zinc oxide nanocatalyst. *Renewable Energy*, 98, 101–107. <https://doi.org/10.1016/j.renene.2016.03.018>
2. Baskar, G., Selvakumari, I. A. E., Aiswarya, R. (2018). Biodiesel production from castor oil using heterogeneous Ni doped ZnO nanocatalyst. *Bioresource Technology*, 250, 793–798. <https://doi.org/10.1016/j.biortech.2017.11.089>
3. Brayko, A., Shigarov, A., Kirillov, V., Kireenkov, V., Kuzin, N., Sobyenin, V., Snytnikov, P., Kharton, V. (2018). Methane partial oxidation over porous nickel monoliths: The effects of NiO–MgO loading on microstructural parameters and hot-spot temperature. *Catalysis Today*, 299, 102–109. <https://doi.org/10.1016/j.cattod.2017.02.019>
4. Darvishvand, H. P., Shabani, N., Farzaneh, F., Azarkamanzad, Z. (2024). The effect of different morphologies of ZnO and Cr doped ZnO NPs as heterogeneous catalyst for biodiesel production from soybean oil.
5. Damian, C. S., Devarajan, Y. (2025). Nanocatalysts in biodiesel production: advancements, challenges, and sustainable solutions. *ChemBioEng Reviews*, 12(2), e202400055.
6. Das, A. (2025). Current progress and difficulties in the application of nanomaterials for biodiesel production. In V. Dave, A. Kuila (Eds.), *Nanomaterials as a catalyst for biofuel production* (pp. xx–xx). Springer. [https://doi.org/10.1007/978-981-96-1706-7\\_1](https://doi.org/10.1007/978-981-96-1706-7_1)
7. Gardy, J., Hassanpour, A., Lai, X., Ahmed, M. H., Rehan, M. (2018). Biodiesel production from used cooking oil using a novel surface functionalised TiO<sub>2</sub> nano-catalyst. *Renewable Energy*, 116, 109–119. <https://doi.org/10.1016/j.renene.2017.08.061>
8. Hara, M. (2009). Environmentally benign production of biodiesel using heterogeneous catalysts. *ChemSusChem*, 2(2), 129–135. <https://doi.org/10.1002/cssc.200800214>
9. Hussain, J., Ali, Z. M., Shah, S. F. A., Laghari, A. N., Sohail, M. (2023). Production of biodiesel from jatropha oil in Pakistan: Current trends and challenges. *Journal of Innovative Sciences*, 9(1), 106–110. <https://dx.doi.org/10.17582/journal.jis/2023/9.1.106.110>
10. Hussain, J., Zeenat, M. A., Khan, M. Q., Nailam, K., Syed, F. A. S. (2022). Production of biodiesel from *Jatropha curcas* by using heterogenous doped zinc oxide. *Journal of Nanoscope*, 3(2), 155–164.
11. Kirubakaran, D. D., Pitchaimuthu, S., Dhas, C. R., Selvaraj, P., Karazhanov, S. Z., Sundaram, S. (2018). Jet-nebulizer-spray coated copper zinc tin sulphide film for low cost platinum-free electrocatalyst in solar cells. *Materials Letters*, 220, 122–125. <https://doi.org/10.1016/j.matlet.2018.03.081>
12. Krawczyk, T. (1996). Biodiesel—Alternative fuel makes inroads but hurdles remain. *Inform*, 7, 800–815.
13. Kumar, U., Gupta, P. (2020). Modeling and optimization of novel biodiesel production from non-edible oil with *Musa balbisiana* root using hybrid response surface methodology along with African

- buffalo optimization. *Reaction Kinetics, Mechanisms and Catalysis*, 130, 875–901. <https://doi.org/10.1007/s11144-020-01807-7>
14. Kurniawan, E., Nurhayati, N. (2020). Transesterification process of waste cooking oil catalyzed by Na/CaO derived from blood clam (*Anadara granosa*) shells. *EKSAKTA: Journal of Sciences and Data Analysis*, 1, 1–6. <https://doi.org/10.20885/EKSAKTA.voll.iss1.art1>
  15. Lin, Y., Hsu, C., Hung, S., Chang, C., Wen, D. (n.d.). The structural and optoelectronic properties of Ti-doped ZnO thin films prepared by introducing a Cr buffer layer and post-annealing. (Please provide complete publication details).
  16. Rajagopal, D. (2007, January). Rethinking current strategies for biofuel production in India. In *International Conference on Linkages in Water and Energy in Developing Countries* 29–30. ICRISAT, Hyderabad, India: IWMI and FAO.
  17. Safaripour, M., Saidi, M., Jahangiri, A. (2023). Application of samarium doped lanthanum nickel oxide perovskite nanocatalyst for biodiesel production. *Energy Conversion and Management*, 296, 117667. <https://doi.org/10.1016/j.enconman.2023.117667>
  18. Sampa, C., Xin, L., Changning, L., Prantik, B., Saikat, M., Mark, T. S. (2015). Synthesis of iron-doped zinc oxide nanoparticles by simple heating: Influence of precursor composition and temperature. *International Journal of Materials Engineering Innovation*, 6(1).
  19. Sathish, M., Viswanath, R. P. (2007). Photocatalytic generation of hydrogen over mesoporous CdS nanoparticle: Effect of particle size, noble metal and support. *Catalysis Today*, 129(3), 421–427. <https://doi.org/10.1016/j.cattod.2007.08.029>
  20. Sharma, S., Hasan, A., Kumar, N., Pandey, L. M. (2018). Removal of methylene blue dye from aqueous solution using immobilized *Agrobacterium fabrum* biomass along with iron oxide nanoparticles as biosorbent. *Environmental Science and Pollution Research*, 25(22), 21605–21615. <https://doi.org/10.1007/s11356-018-2255-x>
  21. Sharma, S., Saxena, V., Baranwal, A., Chandra, P., Pandey, L. M. (2018). Engineered nanoporous materials mediated heterogeneous catalysts and their implications in biodiesel production. *Materials Science for Energy Technologies*, 1(1), 11–21. <https://doi.org/10.1016/j.mset.2018.03.001>
  22. Sudhagar, P., Sathyamoorthy, R., Chandramohan, S., Senthilarasu, S., Lee, S.-H. (2008). Synthesis of  $\text{Cd}_{1-x}\text{Mn}_x\text{S}$  nanoclusters by surfactant-assisted method: Structural, optical and magnetic properties. *Materials Letters*, 62(16), 2430–2433. <https://doi.org/10.1016/j.matlet.2007.11.091>
  23. Yuan, H., Xu, M., Huang, Q. Z. (2014). Effects of pH of the precursor sol on structural and optical properties of Cu-doped ZnO thin films. *Journal of Alloys and Compounds*, 616, 401–407. <https://doi.org/10.1016/j.jallcom.2014.07.040>